

ID1 overexpression promotes HCC progression by amplifying the AURKA/Myc signaling pathway

MAN WU^{1*}, YUHONG ZHOU^{2*}, CHENGMING FEI^{3*}, TIANYI CHEN¹,
XIN YIN¹, LAN ZHANG¹ and ZHENGANG REN¹

¹Liver Cancer Institute and Key Laboratory of Carcinogenesis and Cancer Invasion; ²Department of Oncology, Zhongshan Hospital, Fudan University, Shanghai 200032; ³Department of Hematology, Shanghai Jiao Tong University Affiliated Sixth People's Hospital, Shanghai 200223, P.R. China

Received February 6, 2020; Accepted June 1, 2020

DOI: 10.3892/ijo.2020.5092

Abstract. Hepatocellular carcinoma (HCC) is the fourth most common cancer type worldwide, with a poor prognosis and high mortality rate. The aim of the present study was to investigate the mechanisms underlying HCC progression to potentially benefit the development of effective therapies for advanced HCC. The present study reported a novel mechanism that promotes the HCC malignant phenotype, in which the inhibitor of differentiation 1 (ID1) activates the aurora kinase A (AURKA)/Myc signaling pathway. Specifically, a high expression of ID1 promoted a highly malignant phenotype of HCC cells that exhibit enhanced metastatic ability and drug resistance. However, the effects of ID1 were markedly reversed by the AURKA inhibitor VX689 and the Myc inhibitor 10058-F4. Further studies demonstrated that ID1 competitively binds with anaphase-promoting complex/cyclosome Cdh1 (APC/C^{Cdh1}), which is responsible for ubiquitination-mediated AURKA protein degradation, resulting in upregulation of AURKA. Increased AURKA expression subsequently enhanced Myc expression at both transcriptional and post-transcriptional level, leading to amplification of the Myc oncogenic signaling

pathway. This novel ID1/AURKA/Myc axis could be a promising therapeutic target for the development of effective therapeutic strategies for advanced HCC.

Introduction

Hepatocellular carcinoma (HCC) was the sixth most commonly diagnosed cancer and the third leading cause of cancer-associated mortality worldwide in 2018, with a 5-year relative survival rate of <20% (1). The incidence of HCC is increasing faster than for any other cancer type in both men [5-year average annual percent change (AAPC) = 2.8%] and women (5-year AAPC = 3.8%) (2). Currently, surgical resection or liver transplantation are the only curative treatments for early-stage HCC; however, only a small portion of patients are candidates for these curative treatments as most patients are diagnosed at an advanced stage (3). Transcatheter arterial chemoembolization or systemic chemotherapy have been reported to improve the survival of patients with advanced HCC (4). However, the clinical benefits remain unfavorable, most likely due to HCC malignant progression, such as acquired drug resistance, metastasis and recurrence (5). Therefore, further understanding of the underlying mechanisms is critical for the development of more effective therapies.

Inhibitor of differentiation 1 (ID1), a dominant-negative inhibitor of the basic helix-loop-helix transcription factor, has been reported to mediate diverse cellular functions, including inhibition of differentiation, as well as promotion of cancer neo-angiogenesis and metastasis (6). Increased ID1 expression has been demonstrated to be associated with both cancer progression and poor prognosis in several types of solid human tumors, such as breast, lung, brain and pancreatic cancer (7-11). A previous study proposed that ID1 mediates androgen-stimulated HCC cell migration and invasion (12). In addition, it was previously identified that ID1 confers drug resistance to oxaliplatin or sorafenib in HCC cells (13,14), indicating an important role of ID1 in HCC malignant progression and suggesting ID1 may be a potential target for the treatment of advanced HCC. However, to the best of our knowledge, the precise biological function of ID1 in HCC progression remains largely unknown and there is no effective therapeutic strategy targeting ID1 currently available.

Correspondence to: Dr Zhenggang Ren, Liver Cancer Institute and Key Laboratory of Carcinogenesis and Cancer Invasion, Zhongshan Hospital, Fudan University, Building 16, 180 Fengling Road, Shanghai 200032, P.R. China
E-mail: renzhenggang@hotmail.com

*Contributed equally

Abbreviations: HCC, hepatocellular carcinoma; ID1, inhibitor of differentiation 1; AURKA, aurora kinase A; CHX, cycloheximide; HR, hazard ratio; IC₅₀, half-maximal inhibitory concentration; AKI, AURKA inhibitor; MYCI, Myc inhibitor; APC/CCdh1, anaphase-promoting complex/cyclosome Cdh1; TMA, tissue microarray

Key words: hepatocellular carcinoma, liver cancer, tumor progression, inhibitor of differentiation 1, aurora kinase A, Myc

Aurora kinase A (AURKA), a serine/threonine kinase, is a crucial regulator of cell cycle progression and mitosis (15). A number of studies have reported that AURKA can function as an oncoprotein and therefore may be a promising therapeutic target in various types of malignant tumor, including HCC (15-17). An aberrant high expression of AURKA has been observed in HCC tissues and is significantly correlated with poor prognosis (17). It has been demonstrated that AURKA is involved in uncontrolled proliferation, anti-apoptotic properties and the epithelial-mesenchymal transition in cancer cells, as well as the self-renewal cancer stem cell phenotype (16). Therefore, a number of AURKA inhibitors (AKI) have been produced in the past decades, some of which are already being evaluated in clinical trials (18,19). However, to the best of our knowledge, the mechanism that is responsible for the dysregulation of AURKA expression remains unknown, and no literature has reported the association between ID1 and AURKA in cancer, particularly HCC. Notably, previous studies have reported that ID1 can be localized at centrosomes and is implicated in mitotic regulation, while AURKA is a centrosome-localized mitotic kinase (20-22). Furthermore, overexpression of either ID1 or AURKA results in similar centrosome amplification, suggesting a potential association between ID1 and AURKA (20,23). A previous study investigating nasopharyngeal epithelial cells reported that knockdown of AURKA largely rescued the ID1-induced abnormal mitotic phenotype (24), further supporting the hypothesis that AURKA may participate in the biological function of ID1 in HCC.

The present study identified that ID1 protein is upregulated in HCC and closely associated with tumor recurrence and poor survival in patients with HCC. In addition, the expression levels of ID1 and AURKA were positively correlated. Patients with high expression of both ID1 and AURKA exhibited poor recurrence-free survival and overall survival rates. Further mechanistic studies revealed that the novel downstream AURKA/Myc signaling pathway mediated ID1-induced HCC cell growth, migration, invasion, colony formation and drug resistance, which may promote understanding of HCC progression and provide a novel target to improve the therapeutic treatment strategies for patients with advanced HCC.

Materials and methods

Patients. The present study included 81 patients (67 males and 14 females; mean age, 52±12.6 years) who underwent HCC resection between April 2008 and January 2011 at Fudan University Affiliated Zhongshan Hospital (Shanghai, China). Written informed consent was obtained from each patient. No patient had received any preoperative anticancer therapy. HCC was diagnosed based on the diagnostic criteria issued by the American Association for the Study of Liver Diseases (25), and was staged according to the Barcelona Clinic Liver Cancer staging system (26). The clinical data were collected, including age, sex, Child-Pugh classification, HBsAg, TNM grade, tumor number and tumor diameter (Table I). All patients were followed up until May 2013, with a median follow-up time of 46 months. The present study was approved by the Clinical Research Ethics Committee of Fudan University Affiliated Zhongshan Hospital and carried out in accordance with the Declaration of Helsinki.

Table I. Clinical and pathological characteristics of recruited patients with hepatocellular carcinoma.

Characteristic	No. of patients (%)
Age, years	
<60	59 (72.8)
≥60	22 (27.2)
Sex	
Male	67 (82.7)
Female	14 (17.3)
Child-Pugh classification	
A	81 (100)
HBsAg	
Positive	68 (84.0)
Negative	13 (16.0)
TNM grade	
I	38 (46.9)
II	21 (25.9)
III	22 (27.2)
Tumor thrombus	
Yes	32 (39.5)
No	49 (60.5)
Tumor number	
Single	67 (82.7)
Multiple	14 (17.3)
Tumor diameter, cm	
≤5	35 (43.2)
>5	46 (56.8)
HBsAg, hepatitis B surface antigen.	

Antibodies and reagents. The following antibodies were used: Anti-ID1 (cat. no. ab134163; Abcam), anti-ID1 (cat. no. sc-734; Santa Cruz Biotechnology, Inc.), anti-AURKA rabbit mAb (cat. no. 14475; Cell Signaling Technology, Inc.), anti-AURKA mouse mAb (cat. no. ab13824; Abcam), anti-Myc (cat. no. 9402; Cell Signaling Technology, Inc.), anti-APC/C^{Cdh1} (cat. no. ab3242; Abcam), anti-ubiquitin (cat. no. ab7780; Abcam) and anti-human/mouse GAPDH (cat. no. 60004-1-Ig; ProteinTech Group, Inc.). VX689 (cat. no. S2770) was purchased from Selleck Chemicals. Cycloheximide (CHX; cat. no. 2112) was obtained from Cell Signaling Technology, Inc. BioCoat Matrigel invasion Chambers were obtained from BD Biosciences. Primers for reverse transcription-quantitative PCR (RT-qPCR) were generated by Sangon Biotech Co., Ltd. PrimeScript RT reagent kit (cat. no. DRR037A) and SYBR Premix Ex Taq (cat. no. DRR081) were purchased from Takara Bio, Inc. All chemicals were of reagent grade or higher.

Cell culture, plasmids and transfection. The human HCC cell line MHCC-97H was established at our Liver Cancer Institute in Fudan University Affiliated Zhongshan Hospital (27) and tested for mycoplasma contamination before use. MHCC-97H cells in passages 12-15 were used in the experiments in the

present study. Cells were cultured in Dulbecco's modified Eagle's medium (DMEM; Gibco; Thermo Fisher Scientific, Inc.) supplemented with 10% fetal bovine serum (FBS; Gibco; Thermo Fisher Scientific, Inc.) and 1% antibiotic mixture (penicillin, streptomycin and amphotericin B; Sigma-Aldrich; Merck KGaA) at 37°C in a 5% CO₂ incubator.

MHCC-97H cells with stable ID1 transfection (97H-ID1) were generated using ID1-overexpressing lentiviruses (Shanghai GeneChem Co., Ltd.). MHCC-97H cells were prepared and infected at a multiplicity of infection (MOI) of 10 with empty vector, ID1-overexpressing lentivirus or 3xFlag-tagged AURKA-overexpressing lentivirus (Shanghai GeneChem Co., Ltd.) at 37°C for 24 h. For AURKA-knockdown, short hairpin RNA (shRNA) targeting AURKA was delivered by lentiviral infection into MHCC-97H cells with a MOI of 10 (Shanghai GeneChem Co., Ltd.). After 3 days of transfection, cells were used for subsequent experiments. The sequence of AURKA shRNA was 5'-CATTCTTTGCAAGCACAA-3'. A scrambled shRNA (5'-TTCTCCGAACGTGTACGT-3') was used as the control (Shanghai GeneChem Co., Ltd.).

Immunohistochemistry (IHC) and H-Scoring of tissue microarray (TMA). IHC staining was performed with a TMA consisting of the 81 HCC cases. The TMA was prepared as described previously (28). The TMA section (thickness, 4-μm) was deparaffinized and rehydrated, followed by heat-induced antigen retrieval and blocking with 5% goat serum (Thermo Fisher Scientific, Inc.) at room temperature for 2 h. The section was then incubated with anti-ID1 rabbit antibodies (1:500) or anti-AURKA mouse antibodies (1:200) overnight at 4°C. The following day, the section was washed and incubated with biotin-conjugated anti-mouse (cat. no. B0529; 1:300; Sigma-Aldrich; Merck KGaA) or anti-rabbit secondary antibodies (cat. no. B8895; 1:300; Sigma-Aldrich; Merck KGaA) for 1 h at room temperature. Subsequently, the ABC enhanced Vectastain kit system (Vector Laboratories, Inc.; Maravai LifeSciences), a DAB peroxidase substrate kit (Thermo Fisher Scientific, Inc.) and hematoxylin solution (cat. no. ab220365; Abcam) were used for detection and visualization. Sections were stained with hematoxylin for 2 min at room temperature. Images were obtained using a light microscope (magnification, x200).

The IHC staining was quantified as the H-score, which has been validated in breast cancer (29). Typical images (4 random images per sample) were analyzed and divided into four intensity levels: 0, negative; 1, weak; 2, intermediate; and 3, strong brown staining. The H-score (between 0 and 300) for each sample was calculated as follows: H-score = (% of cells stained at intensity 1 x 1) + (% of cells stained at intensity 2 x 2) + (% of cells stained at intensity 3 x 3). Using the median value of the H-score as a cutoff value, patients with HCC were divided into low and high ID1 or AURKA expression groups. For further analysis, patients were also divided into three groups based on H-scores: i) ID1^{high}AURKA^{high} group; ii) ID1^{high}AURKA^{low}/ID1^{low}AURKA^{high} group; and iii) ID1^{low}AURKA^{low} group.

Cell proliferation assay. Cell proliferation was analyzed using a Cell Counting Kit-8 (CCK-8; Abcam) assay. HCC cells were plated in 96-well plates at a density of 3x10³ cells/well in

DMEM supplemented with 10% FBS and cultured for 1, 2, 3, 4, 5 and 6 days. CCK-8 reagent was then added to each well, according to the manufacturer's instructions. The absorbance at 450 nm of each well was measured using a microplate spectrophotometer.

Tumor cell viability assay. Currently, an oxaliplatin-containing regimen (FOLFOX4), sorafenib and lenvatinib are the first-line chemotherapy drugs for advanced HCC (30). Among them, due to its high efficiency and lower cost, oxaliplatin-containing regimen is the most widely used chemotherapy in the treatment of advanced HCC, particularly in China (31). Furthermore, our previous study demonstrated that ID1 was highly expressed in oxaliplatin-treated HCC tumors and was critical for the chemoresistance of HCC cells to oxaliplatin (13). Therefore, to investigate the mechanism underlying ID1-promoted chemoresistance, the present study used oxaliplatin to analyze the drug sensitivity of HCC cells. Cells were plated in 96-well plates at a density of 1x10⁴ cells/well and exposed to oxaliplatin (Sigma-Aldrich; Merck KGaA) at increasing concentrations (0, 5, 10, 50, 100 and 150 μmol/l) at 37°C for 48 h. The CCK-8 reagent was then added to each well according to the manufacturer's instructions. The absorbance of each well was measured at 450 nm using a microplate. Based on results of three independent experiments, the half-maximal inhibitory concentration (IC₅₀) was calculated for each group.

Tumor cell invasion assay. Invasion of tumor cells was examined by Transwell assay with BioCoat Matrigel invasion Chambers (pore size, 8-μm). Cells (4x10⁴ cells per chamber) were seeded in serum-free medium in the upper chamber, and 10% FBS was used as chemoattractant in the lower chamber. Cells were then cultured for 24 h, and the invasive cells were stained with 0.05% crystal violet at room temperature for 20 min and images were obtained using a light microscope (magnification, x200). Experiments were repeated at least three times.

Tumor cell migration assay. The wound healing assays were performed according to the methods described by Slevin *et al* (32). MHCC-97H and 97H-ID1 cells were separately grown on cover slips in 6-well plates to 100% confluence, and monolayers were then scratched to form a wound area using 200-μl sterile pipette tips. MHCC-97H cells were then cultured with DMEM containing 1% FBS, and 97H-ID1 cells were cultured with solvent control or 250 nM VX689 for a further 24 h. Cells were fixed with 4% formalin at room temperature for 1 h, and images were captured by light microscope (magnification, x100). Experiments were repeated at least three times.

Cell colony formation assay. HCC cells were plated at a density of 1x10³ cells/well in 6-well plates and cultured with DMEM containing 1% FBS. Culture medium was changed every 3 days, and the colonies were stained with 5% Giemsa stain at room temperature for 20 min and images were obtained using a camera. Quantification was performed using Image-Pro plus v5.0 (Media Cybernetics, Inc.). Experiments were repeated at least three times.

Table II. Primers for reverse transcription-quantitative PCR.

Gene	Primer sequence (5'→3')	
	Forward	Reverse
ID1	ACACAAGATGCGATCGTCC	GGAATCCGAAGTTGGAACC
AURKA	TTCAGGACCTGTTAAGGCTACA	ATTTGAAGGACACAAGACCCG
MYC	GGAGGCTATTCTGCCCCATTG	CGAGGTCATAGTTCCTGTTGGTG
GAPDH	GGTGGTCTCCTCTGACTTCAACA	GTTGCTGTAGCCAAATTCGTTGT

AURKA, aurora kinase A; ID1, inhibitor of differentiation 1.

RT-qPCR. Total RNA was isolated from HCC cells using TRIzol reagent (Invitrogen; Thermo Fisher Scientific, Inc.) and reverse-transcribed to cDNA using PrimeScript RT reagent kit according to the manufacturer's instructions. For qPCR, SYBR Premix Ex Taq was used according to the manufacturer's instructions. The thermocycling conditions were as follows: 95°C for 30 sec; followed by 40 cycles of 95°C for 5 sec and 60°C for 20 sec; and 95°C for 15 sec. The primers used for qPCR are listed in Table II. The $2^{-\Delta\Delta C_q}$ method was used for quantification (33). GAPDH was used as the reference gene.

Western blotting, pulse-chase analysis, ubiquitination analysis and co-immunoprecipitation assay. Western blot analysis was performed as previously described (34). A BCA kit (Thermo Fisher Scientific, Inc.) was used for protein determination, and 30 μ g cell lysates were separated by 10% SDS-PAGE and transferred to nitrocellulose membranes (Thermo Fisher Scientific, Inc.) using the iBlot gel transfer device (Thermo Fisher Scientific, Inc.). The membranes were separately blotted with primary antibodies (1:1,000) against ID1, AURKA, Myc or APC/C^{Cdh1} at 4°C overnight, and were subsequently incubated with HRP-conjugated anti-mouse or anti-rabbit secondary antibodies (cat. nos. ab205719 and ab205718; Abcam; 1:5,000) at room temperature for 1 h. For pulse-chase analysis, CHX was used to inhibit protein production. Cells were treated with 25 mmol/l CHX at 37°C for 0, 1, 2, 4, 6, and 8 h, then the cell lysates were subjected to western blot analysis. Image J 1.43 software (National Institutes of Health) was used for densitometric analysis. For ubiquitination analysis, cells were pretreated with 10 μ mol/l MG132 at 37°C for 6 h to inhibit proteasome-mediated proteolysis, followed by immunoprecipitation and western blot analysis. For the co-immunoprecipitation assay, cells were directly lysed with lysis buffer (Tris-HCl, 50 mmol/l, pH 8.0; NaCl, 150 mmol/l; EDTA, 5 mmol/l; 0.5% NP-40). Lysates (1 mg) were then incubated with 1 μ g primary antibodies against ID1 or AURKA on a rotating wheel at 4°C overnight and then pulled down using protein A/G agarose beads at 4°C for 6 h. Beads were collected by centrifugation at 200 x g for 2 min at 4°C and washed 5 times with ice-cold PBS buffer, and then boiled in 2 x SDS-PAGE electrophoresis sample buffers, following by western blot analysis.

Oncomine database analysis. The Oncomine 4.5 database (www.oncomine.org), a publicly available database of published cancer gene expression profiles, was queried for

alterations in ID1 and AURKA gene expression in HCC. The Cancer Genome Atlas (TCGA; www.cancer.gov), Guichard_Liver (35) and Lamb JR_Liver DNA (36) datasets were retrieved for further analysis, comparing the difference between HCC and normal tissues, as well as the correlation between ID1 and AURKA. Data were log-transformed and median-centered, and all statistical analyses were performed using functions implemented in Oncomine.

Statistical analysis. All quantified data are presented as mean \pm standard deviation. Statistical analysis was performed using SPSS v22.0 (IBM Corp.). Differences between two groups were analyzed using an unpaired Student's t-test. Differences among three or more groups were analyzed by one-way analysis of variance followed by Tukey's multiple comparison test. In addition, data in the 2x2 contingency table were analyzed by χ^2 test. Pearson's correlation analysis was performed to determine the correlation between ID1 and AURKA DNA levels. Differences in survival curves were analyzed by Kaplan-Meier analysis and a log-rank test. All data presented are representative of three independent experiments. $P < 0.05$ was considered to indicate a statistically significant difference.

Results

Patients with HCC exhibit an overexpression of ID1, which is associated with poor prognosis. To reveal the ID1 expression pattern in HCC, ID1 expression was first analyzed in TCGA, Guichard_Liver and Lamb JR_Liver DNA datasets. Oncomine analysis revealed a significantly higher expression level of ID1 gene in HCC compared with normal tissues ($P < 0.001$; Fig. 1A). Survival analysis using the Guichard_Liver dataset revealed that a high expression of ID1 gene was significantly associated with a poor recurrence-free survival rate [hazard ratio (HR), 1.865; $P < 0.05$] and low overall survival rate (HR, 2.035; $P < 0.05$; Fig. 1B). To determine whether this association also existed at the protein level, IHC staining was performed with a human HCC TMA, which included tissues obtained from 81 patients with HCC undergoing surgical resection. The clinical and pathological information of the patients is presented in Table I. It was revealed that ID1 was mostly located in the cytoplasm and sometimes located in the nucleus and the area surrounding it (data not shown). According to the expression intensity of ID1, IHC results were divided

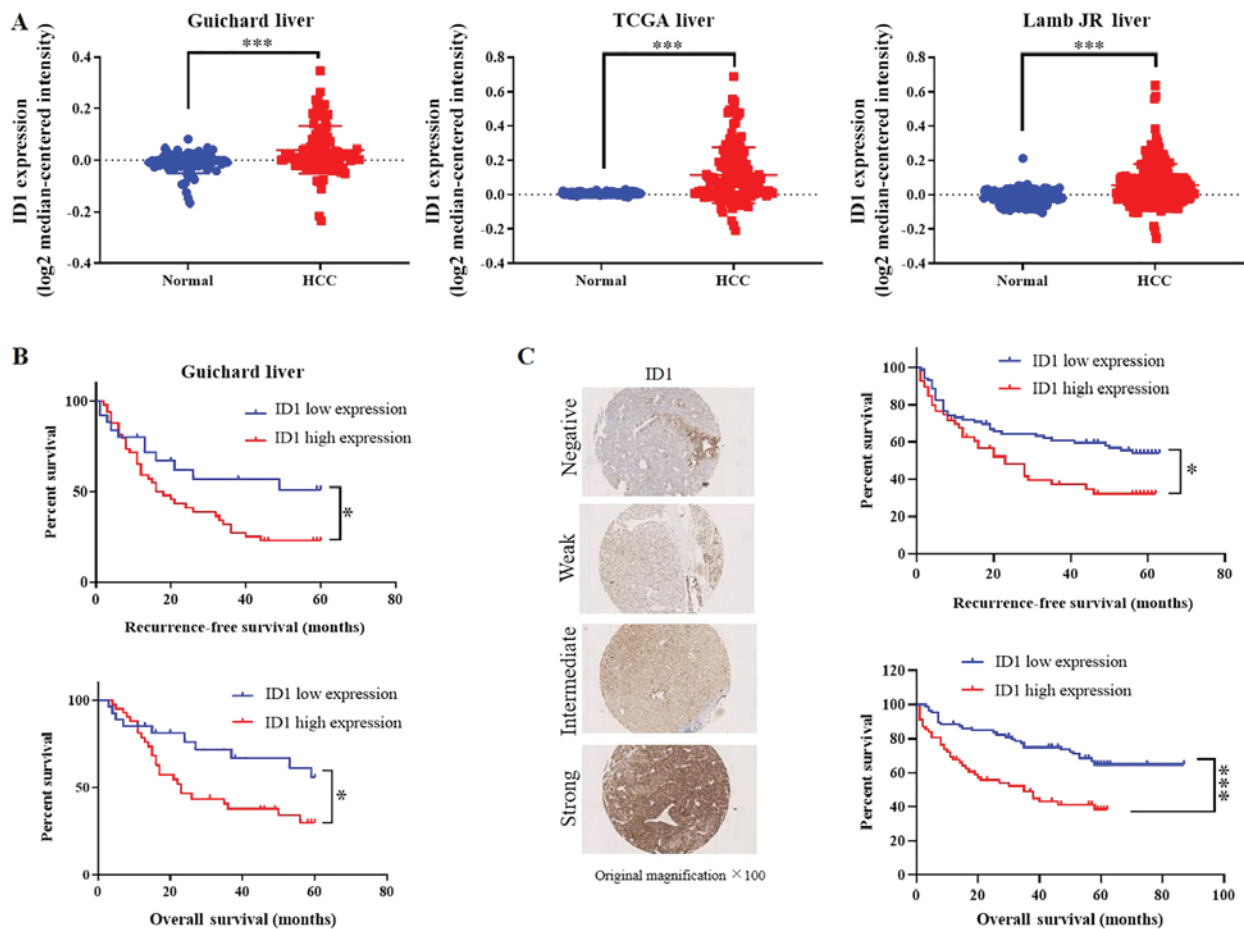


Figure 1. Association of ID1 expression with poor prognosis of patients with HCC. (A) Analysis of three independent genetic datasets obtained from the Oncomine public database revealed a significant increase of ID1 DNA expression level in patients with HCC compared with healthy controls. (B) Survival analysis of the Guichard_Liver DNA dataset revealed a significant association of high ID1 expression level with poor recurrence-free survival and short overall survival for patients with HCC patients. (C) IHC staining of ID1 protein expression levels in a human tissue microarray consisting of 81 HCC cases. Magnification, x100. The immunohistochemistry staining was quantified as the H-score. Using the median value of the H-score as a cutoff value, HCC patients were divided into low (n=41) and high (n=40) ID1 expression groups. Survival analysis revealed that high ID1 protein level was significantly associated with short overall survival and poor recurrence-free survival for patients with HCC. *P<0.05, ***P<0.001. HCC, hepatocellular carcinoma; ID1, inhibitor of differentiation 1; TCGA, The Cancer Genome Atlas.

into four intensity levels: Negative, weak, intermediate, and strong (Fig. 1C). Survival analysis based on the H-score was then performed. This demonstrated that the ID1 protein level was also significantly associated with a poor recurrence-free survival rate (HR, 1.831; P<0.05) and low overall survival rate (HR, 2.397; P<0.0001; Fig. 1C). These results implied that ID1 was a risk factor for poor prognosis and most likely facilitated HCC progression.

Positive correlation of ID1 and AURKA in patients with HCC and the clinical relevance. Given the close interaction between ID1 and AURKA in nasopharyngeal epithelial cells (24), the present study investigated whether this close association also exists in HCC by analyzing the three aforementioned independent DNA datasets. Notably, a significant positive correlation was identified between ID1 and AURKA in all three datasets (P<0.0001; Fig. 2A). To confirm these results and further elucidate the clinical relevance of ID1 and AURKA expression in HCC, AURKA expression was measured in the 81 HCC samples by IHC staining (Fig. 2B). Similar to ID1, AURKA was mostly located in the cytoplasm (data not shown). Consistently,

survival analysis revealed that the protein level of ID1 was significantly associated with AURKA expression (P<0.05; Fig. 2C). Furthermore, the patients with HCC were divided into three groups based on H-scores: i) ID1^{high}AURKA^{high} group (n=29); ii) ID1^{high}AURKA^{low}/ID1^{low}AURKA^{high} group (n=30); and iii) ID1^{low}AURKA^{low} group (n=22). Survival analysis demonstrated a significant difference among all three groups (P<0.0001). Additionally, compared with the ID1^{low}AURKA^{low} group, patients in ID1^{high}AURKA^{high} group had a significantly lower overall survival rate (HR, 4.801; P<0.0001) and recurrence-free survival rate (HR, 4.084; P<0.0001), indicating that high expression of both ID1 and AURKA was associated with an unfavorable prognosis in HCC (Fig. 2D).

Overexpression of ID1 significantly promotes HCC cell proliferation, migration, invasion, colony formation and chemoresistance against oxaliplatin. To investigate the functional mechanism of ID1 in HCC malignant progression, a stable ID1-overexpressing cell line (97H-ID1) was established. The successful establishment of 97H-ID1 was confirmed by western blotting (Fig. 3A). Our previous study demonstrated

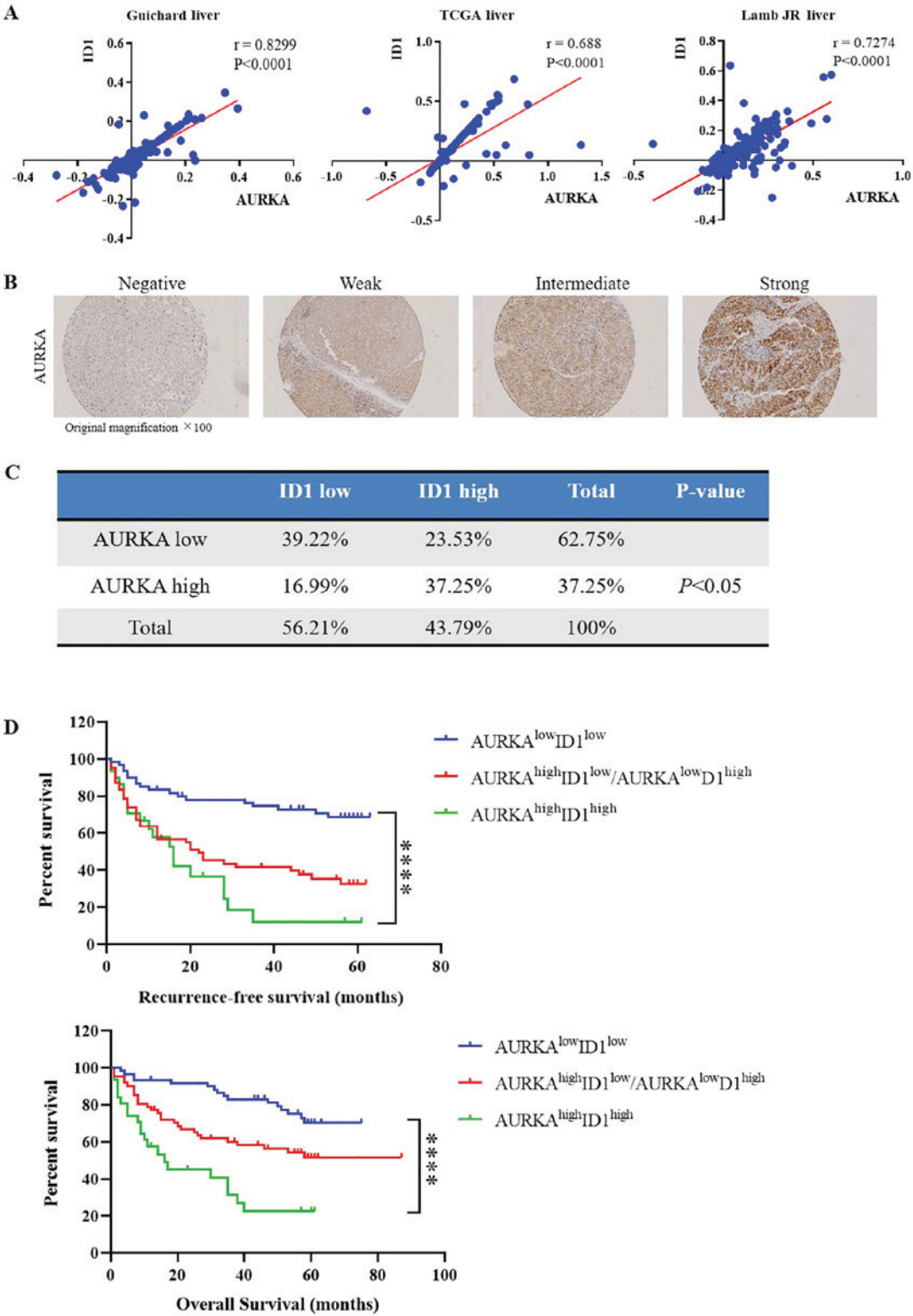


Figure 2. Positive correlation between ID1 and AURKA in patients with HCC and its clinical relevance. (A) Analysis of three independent datasets obtained from the Oncomine public database demonstrated a positive correlation between ID1 and AURKA in patients with HCC. P-value was obtained by Pearson's correlation analysis. (B) Immunohistochemistry staining results of AURKA protein in a TMA consisting of the 81 patients with HCC. Magnification, ×100. (C) Correlation between ID1 and AURKA protein levels in HCC patients. P-value was obtained by χ^2 test. (D) Survival analysis was performed based on the H-scores of ID1 and AURKA in the HCC TMA. High expression of both ID1 and AURKA (ID1^{high}AURKA^{high}) predicted a poorer prognosis, with short overall survival and recurrence-free survival. **** $P < 0.0001$. TMA, tissue microarray; HCC, hepatocellular carcinoma; ID1, inhibitor of differentiation 1; AURKA, aurora kinase A; TCGA, The Cancer Genome Atlas.

that silencing ID1 expression inhibits oxaliplatin-resistant HCC cell proliferation, clone formation and chemoresistance (13). Consistently, the present study demonstrated that, compared

with the control cells, 97H-ID1 cells were more resistant to oxaliplatin (Fig. 3B), with an IC_{50} value of $45.3 \pm 5.65 \mu\text{mol/l}$ in control cells compared with $165.4 \pm 14.12 \mu\text{mol/l}$ in 97H-ID1

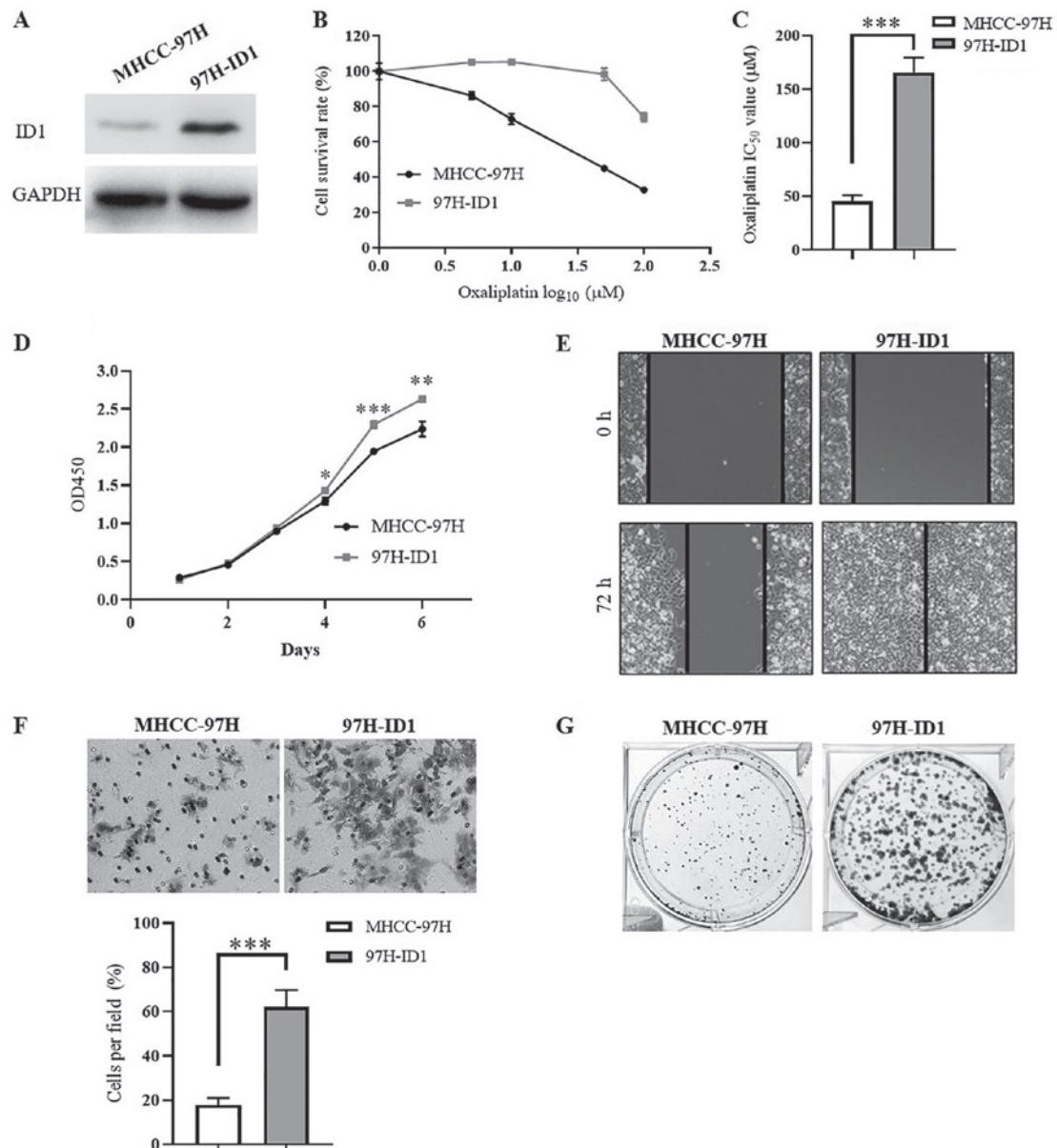


Figure 3. ID1 promotes HCC cell proliferation, migration, invasion, colony formation and chemoresistance. (A) Western blot analysis confirmed the successful establishment of ID1-overexpressing HCC cells (97H-ID1). (B) Results of CCK-8 assay demonstrated the different cytotoxic effects of oxaliplatin on 97H-ID1 cells and the parental cells MHCC-97H. (C) Statistical analysis revealed a significant difference in the IC₅₀ of oxaliplatin in 97H-ID1 and MHCC-97H cells. ***P<0.001. (D) CCK-8 assay revealed that ID1 overexpression significantly promoted HCC cell proliferation at days 4-6. *P<0.05, **P<0.01, ***P<0.001 vs. MHCC-97H cells. (E) Wound healing assay demonstrated an increase of cell migration induced by ID1 overexpression. Magnification, x100. (F) Transwell invasion assay showed that ID1 overexpression significantly enhanced HCC cell invasion through Matrigel. ***P<0.001. Magnification, x200. (G) ID1 overexpression facilitated the ability of HCC cells to form colonies. Each experiment was repeated independently at least three times. HCC, hepatocellular carcinoma; ID1, inhibitor of differentiation 1; CCK-8, Cell Counting Kit-8; IC₅₀, half-maximal inhibitory concentration; OD, optical density.

cells (P<0.001; Fig. 3C). In addition, it was identified that ID1 overexpression significantly promoted HCC cell proliferation at days 4-6 (P<0.05; Fig. 3D). Furthermore, ID1 overexpression markedly enhanced HCC cell migration (Fig. 3E), invasion (P<0.001; Fig. 3F) and colony formation (Fig. 3G). These results further indicated that ID1 promotes HCC malignant progression, contributing to tumor expansion, metastasis and recurrence, which partially explains the close association of ID1 with adverse clinical prognosis.

AURKA mediates the ID1-induced HCC cell malignant progression. Based on the positive correlation identified between ID1 and AURKA in HCC, it was speculated that

AURKA may be involved in ID1-induced HCC cell progression. Notably, it was identified that, along with an increased ID1 expression, AURKA expression was also increased in 97H-ID1 cells compared with MHCC-97H cells (Fig. 4A). To verify if AURKA mediates ID1-induced HCC malignant progression, a highly selective AKI VX689 was used (Fig. 4B). Compared with the control, 250 nM VX689 significantly reversed the ID1-induced resistance to oxaliplatin in 97H-ID1 cells (Fig. 4C), with the IC₅₀ of oxaliplatin in 97H-ID1 cells decreasing from 162.1±10.63 to 54.73±8.45 μmol/l following treatment with VX689 (P<0.001; Fig. 4C). To address the chemosensitizer role of AKI, different concentrations were evaluated (data not shown) and a low dose (250 nM) of VX689

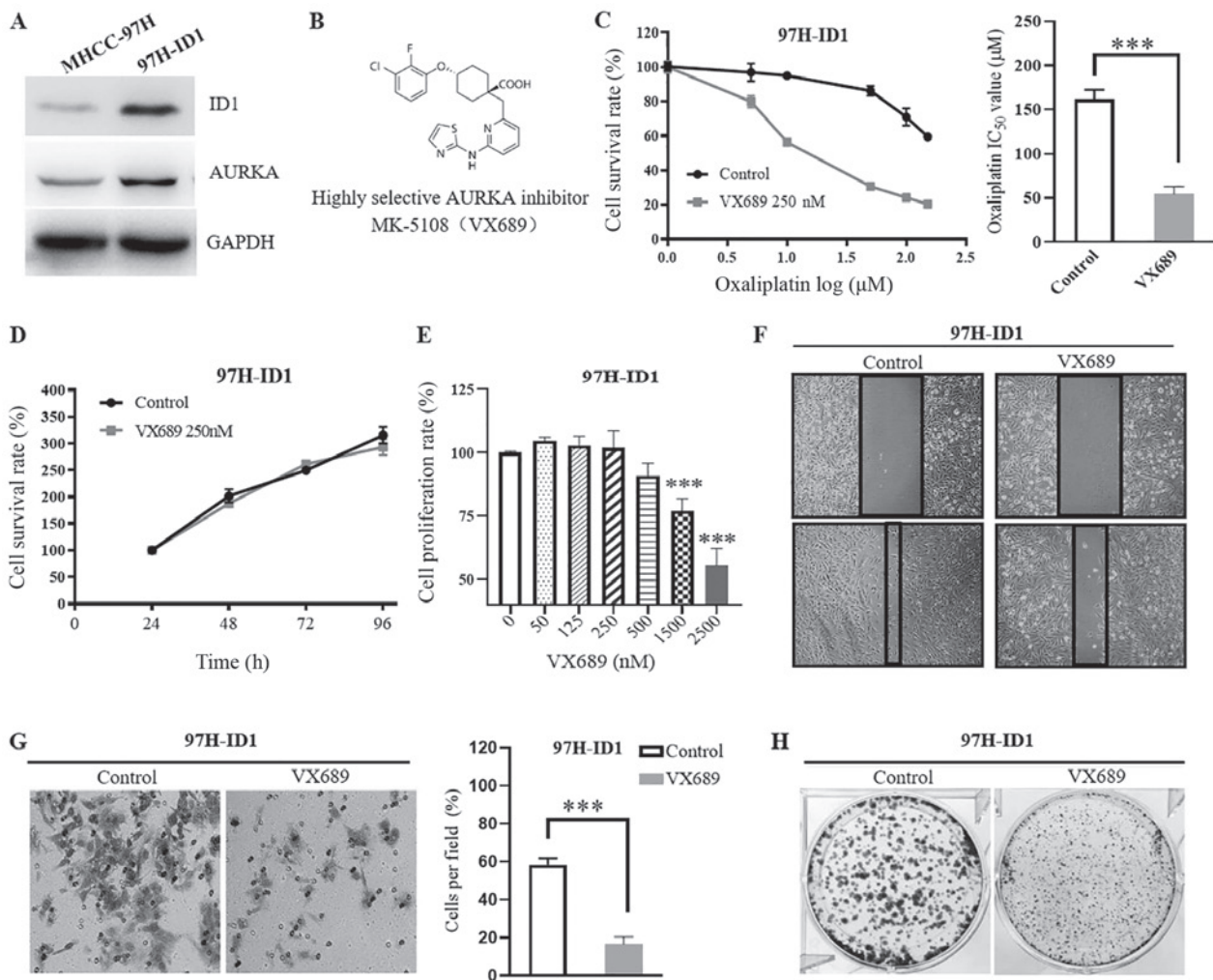


Figure 4. AURKA mediates ID1-induced HCC cell malignant progression. (A) Western blotting revealed an increased expression of AURKA protein in 97H-ID1 cells. (B) Structural formula of the highly selective AURKA inhibitor MK-5108, also known as VX689. (C) Co-treatment with 250 nM AURKA inhibitor VX689 for 48 h reversed the ID1-induced chemoresistance to oxaliplatin. Statistical analysis revealed that addition of 250 nM VX689 significantly decreased the IC₅₀ value of oxaliplatin in 97H-ID1 cells. ****P*<0.001. (D) Treatment with 250 nM VX689 alone had no cytotoxic effect on 97H-ID1 cells. (E) Cell Counting Kit-8 assay revealed the effects of different concentrations of VX689 on HCC cell proliferation. A low dose of VX689 (≤ 500 nM) had no significant effect on HCC cell proliferation, while a high dose ($\geq 1,500$ nM) significantly inhibited cell growth. ****P*<0.001 vs. 0 nM VX689. VX689 at a low concentration (250 nM) could inhibit ID1-enhanced HCC (F) migration (magnification, $\times 100$), (G) colony formation and (H) invasion (magnification, $\times 200$). ****P*<0.001. AURKA, aurora kinase A; ID1, inhibitor of differentiation 1; HCC, hepatocellular carcinoma; 97H-ID1 cells, ID1-overexpressing MHCC-97H cells; IC₅₀, half-maximal inhibitory concentration.

was selected. This dose alone had no cytotoxic effect on HCC cell viability (*P*>0.05; Fig. 4D), which excludes the possibility that the increased sensitivity to oxaliplatin was due to a direct cytotoxic effect of VX689 itself. In addition, it was identified that VX689 significantly inhibited 97H-ID1 cell proliferation at concentrations $\geq 1,500$ nM (*P*<0.0001; Fig. 4E), while concentrations ≤ 500 nM had no significant effect at day 5. However, treatment with 250 nM VX689 impaired the ID1-promoted HCC cell migration (Fig. 4F), invasion (*P*<0.001; Fig. 4G) and colony formation (Fig. 4H), suggesting that the malignant biological phenotypes induced by ID1 are largely dependent on the activation of AURKA.

ID1 upregulates AURKA via inhibition of AURKA proteolysis degradation. Since ID1 expression was correlated with AURKA protein expression in HCC, the present study further analyzed whether ID1 could transcriptionally activate AURKA. Notably, no significant change in AURKA mRNA

level was observed in 97H-ID1 cells compared with control cells (Fig. 5A), indicating that the regulation of ID1 on AURKA may be at the protein level. Pulse-chase analysis results demonstrated that ID1 overexpression significantly impeded AURKA protein degradation (*P*<0.01; Fig. 5B). As E3 ubiquitin ligase-mediated lysine 48 (K48) polyubiquitination and subsequent proteasomal degradation predominantly controls AURKA protein turnover (37,38), the present study analyzed the K48 ubiquitination level of AURKA protein. Consistently, ID1 markedly decreased the ubiquitination of AURKA protein (Fig. 5C). A previous study reported that anaphase-promoting complex/cyclosome Cdh1 (APC/C^{Cdh1}) directly binds with AURKA, initiating the process of ubiquitination-mediated AURKA degradation; and depletion of APC/C^{Cdh1} expression results in stabilization of AURKA protein, indicating a crucial role of APC/C^{Cdh1} in AURKA protein degradation (37). Since ID1 has been reported to bind with APC/C-associated protein Cdc20 (39), it was speculated that ID1 may also

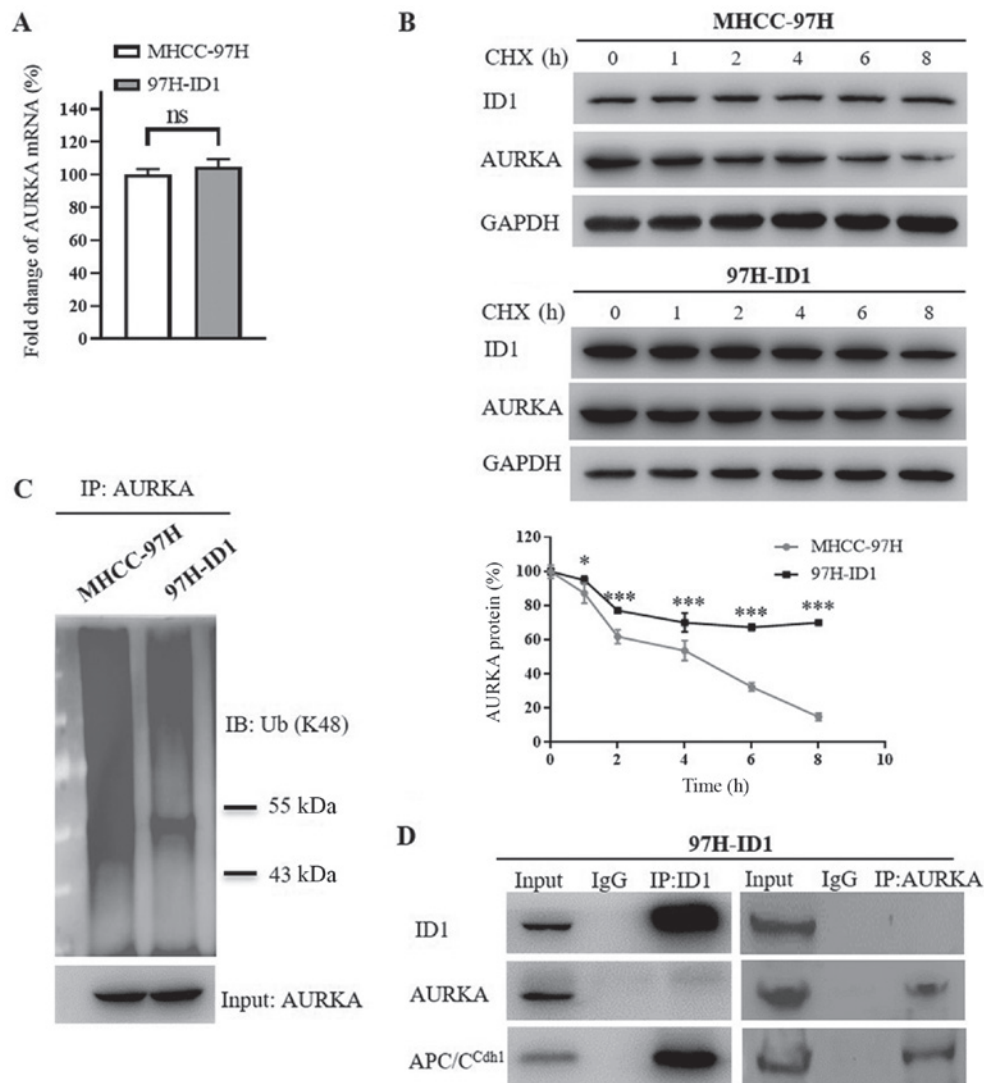


Figure 5. ID1 upregulates AURKA expression by competitively binding with APC/CCdh1, and thus inhibiting AURKA protein degradation. (A) Reverse transcription-quantitative PCR demonstrated that ID1 overexpression had no significant effect on AURKA mRNA expression level. (B) Pulse-chase analysis demonstrated that ID1 overexpression inhibited the proteolysis degradation of AURKA protein. The degradation profile of AURKA protein was examined by blocking protein synthesis with CHX for the indicated times. The AURKA protein levels were examined by western blotting, and the plot represents the AURKA protein degradation rates. *P<0.05, ***P<0.001 vs. MHCC-97H cells. (C) Decreased K48 ubiquitination of AURKA protein induced by ID1 overexpression. To detect the levels of ubiquitinated AURKA, proteasome inhibitor MG132 was used to inhibit AURKA proteolysis, then AURKA protein was pulled down by specific a AURKA antibody. The cell pellets were analyzed using antibodies against K48 ubiquitin. The input level of AURKA protein was shown as reference. (D) Co-immunoprecipitation assay revealed that both ID1 and AURKA directly interact with APC/CCdh1, which is responsible for the ubiquitin-mediated proteasomal-dependent degradation of AURKA. No direct binding between ID1 and AURKA was found. ns, no significance; AURKA, aurora kinase A; ID1, inhibitor of differentiation 1; HCC, hepatocellular carcinoma; 97H-ID1 cells, ID1-overexpressing MHCC-97H cells; APC/CCdh1, anaphase-promoting complex/cyclosome Cdh1; ns, no significance; CHX, cycloheximide; IB, immunoblotting.

interact with APC/CCdh1. A co-immunoprecipitation assay revealed that, similar to AURKA, ID1 was a direct binding partner of APC/CCdh1 in HCC cells (Fig. 5D), while ID1 and AURKA did not bind with each other, suggesting that ID1 may stabilize AURKA indirectly by competitive binding with APC/CCdh1. Taken together, these results revealed a novel mechanism in which excessive ID1 competitively inhibits APC/CCdh1-mediated AURKA protein degradation, leading to upregulation of AURKA.

AURKA promotes Myc expression by facilitating its mRNA expression and simultaneously inhibiting its protein degradation. The oncoprotein Myc, which represents a central hub of pro-tumorigenic signaling networks, is frequently

hyperactivated and implicated in the pathogenesis of several types of human cancer, including HCC (40). In light of the close association of AURKA with Myc family members (41,42), and our previous study that indicated that knockdown of ID1 downregulates Myc expression (13), it was speculated that AURKA may activate the Myc pathway to induce the biological effects of ID1 in HCC. The present results demonstrated that, accompanied with increased AURKA levels, ID1 overexpression also led to a marked upregulation of Myc expression in HCC cells (Fig. 6A). To reveal whether Myc is involved in the biological function of ID1, the Myc inhibitor (MYCI) 10058-F4 was used. Notably, addition of 100 μ M MYCI impaired ID1-mediated HCC cell chemoresistance (Fig. 6B). The IC₅₀ value of oxaliplatin in 97H-ID1 cells decreased from 160.8 \pm 17.19 to 107.6 \pm 5.97 μ mol/l

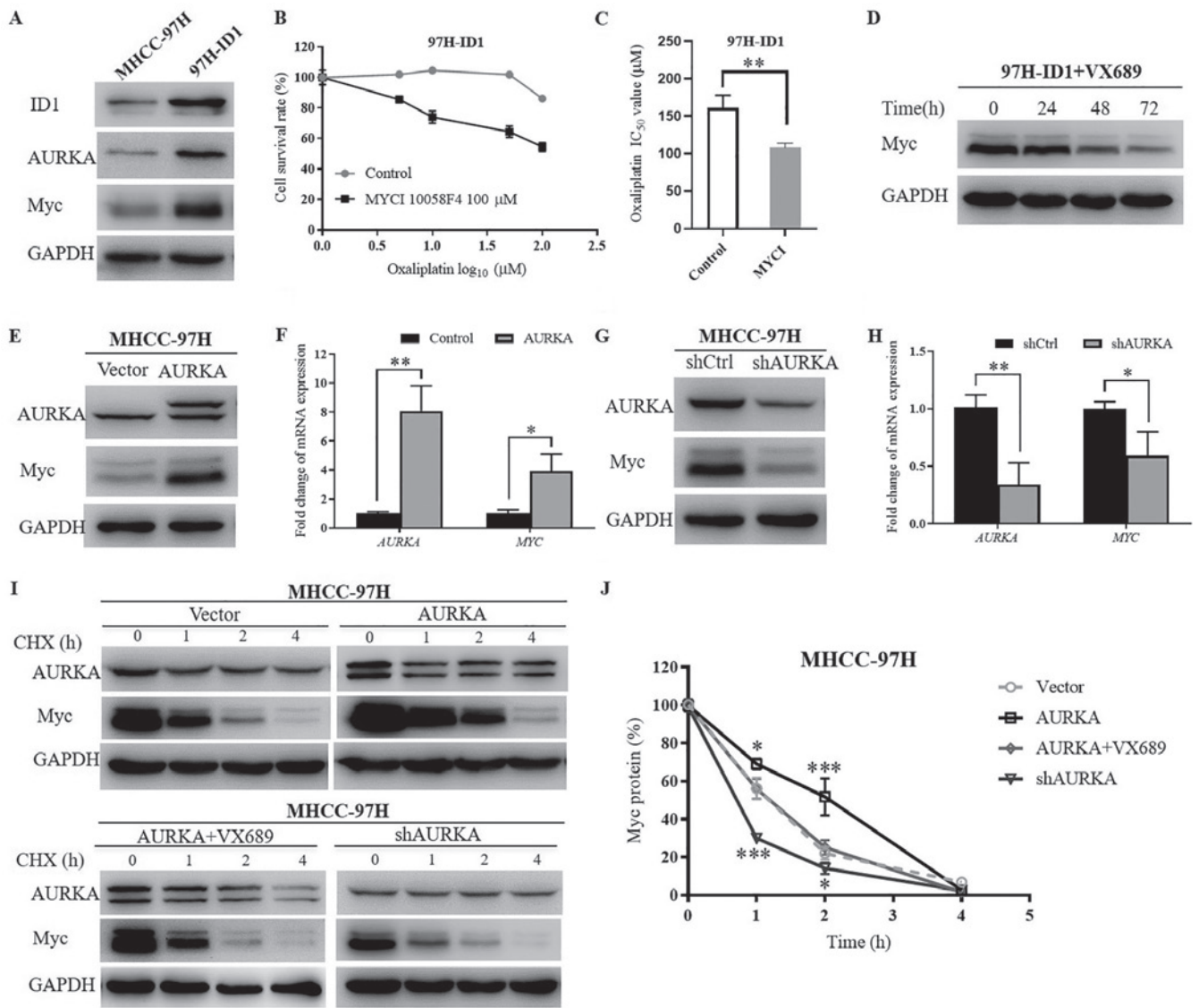


Figure 6. ID1-upregulates the AURKA-induced Myc signaling pathway at both the transcriptional and post-transcriptional levels. (A) Western blotting demonstrated that ID1 overexpression increased AURKA and Myc levels. (B) Addition of 100 μM MYCI (10058-F4) for 48 h impeded ID1-induced HCC chemoresistance to oxaliplatin. (C) Statistical analysis of the IC₅₀ values of oxaliplatin in 97H-ID1 cells with or without MYCI treatment. **P<0.01. (D) AURKA inhibitor VX689 reversed ID1-upregulated Myc expression. (E) Western blotting demonstrated the effect of AURKA overexpression on Myc protein levels. The extra larger-size band of AURKA in AURKA-overexpressing cells was due to the transfection of a 3xFlag-tagged AURKA-overexpression lentivirus. (F) Reverse transcription-quantitative PCR revealed the effect of AURKA overexpression on Myc mRNA expression. (G) Effect of AURKA-knockdown on Myc protein levels. (H) Effect of AURKA knockdown on Myc mRNA expression. *P<0.05, **P<0.01. (I) AURKA expression effected the protein stability of Myc. Pulse-chase analysis of Myc protein stability was performed under conditions of AURKA-overexpression alone, AURKA-overexpression with AURKA inhibitor VX689, or AURKA-knockdown. Parental cells MHCC-97H were used as a control. (J) Statistical analysis of Myc protein degradation rates. *P<0.05, ***P<0.001 vs. vector. AURKA, aurora kinase A; ID1, inhibitor of differentiation 1; HCC, hepatocellular carcinoma; 97H-ID1 cells, ID1-overexpressing MHCC-97H cells; MYCI, Myc inhibitor; IC₅₀, half-maximal inhibitory concentration; shRNA, short hairpin RNA.

following the addition of MYCI (P<0.01; Fig. 6C), verifying that Myc activation is a critical downstream signaling pathway of ID1.

Notably, it was identified that treatment with AKI VX689 markedly decreased Myc expression over time in 97H-ID1 cells, implying that ID1 regulates Myc expression via modulating AURKA (Fig. 6D). To further reveal how AURKA regulates Myc expression, MHCC-97H cells with AURKA overexpression or knockdown were established. The extra larger-size band of AURKA protein in AURKA-overexpressing cells was due to the transfection of a 3xFlag-tagged AURKA vector. The molecular size of the 3xFlag-tag was ~3 kD. Consistent with the previous hypothesis, it was identified that AURKA overexpres-

sion upregulated Myc, while knockdown of AURKA decreased its protein levels (Fig. 6E and G). RT-qPCR demonstrated similar trends that AURKA overexpression resulted in a significant increase of Myc mRNA level, whereas knockdown of AURKA significantly reduced the mRNA level of Myc (Fig. 6F and H). Notably, pulse-chase analysis revealed that AURKA also affected Myc protein stability. Specifically, overexpression of AURKA retarded Myc protein degradation, which could be reversed by addition of 250 nM VX689. In addition, knockdown of AURKA significantly facilitated the degradation of Myc protein (Fig. 6I and J). Collectively, these results demonstrated a novel downstream AURKA/Myc signaling pathway that mediates ID1-promoted HCC cell malignant progression.

Discussion

Acquired chemoresistance and metastasis account for the majority of the treatment failure in HCC (3,43). However, the precise molecular mechanism underlying HCC malignant progression remains largely unknown, which severely hinders the improvement of therapeutic efficacy. The present study demonstrated that ID1 protein was upregulated in HCC tumor tissues and positively associated with early relapse and poor prognosis of patients with HCC. Furthermore, it was identified that the novel downstream AURKA/Myc signaling played a role in ID1-promoted HCC cell growth, migration, invasion and chemoresistance. Blocking either AURKA or Myc could largely reverse ID1-induced HCC malignant progression. Further mechanistic studies revealed that ID1 competitively bound with APC/C^{Cdh1} and inhibited APC/C^{Cdh1}-mediated AURKA protein degradation, thus resulting in increased AURKA expression, which subsequently enhanced the Myc-activated protumorigenic signaling networks.

Aberrant overexpression of ID1 has previously been reported in multiple human cancers and is closely associated with poor survival (11,39). However, little is known regarding the expression pattern of ID1 and its biological function in HCC. Our previous study based on TCGA database revealed that a higher gene expression of ID1 predicted a poorer prognosis in patients with HCC (13). In the present study, by using a human HCC TMA, it was demonstrated that ID1 protein levels were upregulated in HCC and positively associated with tumor recurrence and unfavorable survival. TMA, which was first reported by Kononen *et al* (44), has been long demonstrated to be an effective and efficient tool for immunohistochemical and molecular studies. Although few researchers claim that TMA may not be indicative of the entire sample due to the small size of tissue sections, numerous studies have reported good concordance between tissue microarray spots and whole sections in IHC studies of multiple tumor types (45-47). Generally, the present results largely support that ID1 is an important prognostic factor and is closely involved in HCC pathology.

Abnormal proliferation, migration and invasion are important hallmarks of cancer (48). Our previous study clarified that silencing ID1 inhibits oxaliplatin-resistant HCC cell proliferation, clone formation and chemoresistance (13). In addition, Cho *et al* (49) reported that downregulation of ID1 by small interfering RNA significantly decreases HCC cell invasion. The present study identified that ID1 overexpression significantly promoted aggressive behaviors of MHCC-97H cells, including increased proliferation, migration, invasion, and colony formation. In addition, it was demonstrated that ID1 reduced the sensitivity of HCC cells to oxaliplatin, which partially explained the close association of ID1 with adverse clinical outcomes in patients with HCC. These results further supported the hypothesis that ID1 plays a pivotal role in priming the aggressive behaviors of HCC cells. However, to the best of our knowledge, currently no effective inhibitor targeting ID1 is available. Therefore, further understanding of the functional mechanisms and the downstream signaling of ID1 is urgently required.

A number of studies have reported that AURKA serves an important role in regulating the phenotypes of numerous different cancer cells (16,50-53). However, the regulatory mechanism of AURKA is largely unknown. Notably, the current

study identified that ID1 overexpression significantly increased AURKA expression in HCC cells, and the AKI VX689 reversed ID1-induced HCC cell growth, migration, invasion, colony formation and chemoresistance, indicating that AURKA mediates the ID1-induced HCC cell malignant progression. A previous study reported that ID1 can weakly activate the AURKA promoter in nasopharyngeal epithelial cells (24), whereas, in the present study, no significant change in AURKA mRNA levels was observed in ID1-overexpressing HCC cells, which may be due to different cell types. In addition to the transcriptional activation, AURKA level is also reported to be controlled by ubiquitination-mediated proteasomal degradation. Previous studies have shown that in somatic cells, AURKA is degraded during mitotic exit by the anaphase-promoting complex, which requires APC/C^{Cdh1} as the coactivator (37,38). APC/C^{Cdh1} recognizes and binds with its substrates, such as AURKA, and then initiates ubiquitination, leading to ubiquitin-mediated proteasomal degradation (37). Notably, ID1 has been reported to bind with APC/C-associated protein Cdc20 (39), and a previous report claimed that ID1 and APC/C^{Cdh1} may be binding partners in nasopharyngeal epithelial cells (24). Notably, the present study revealed that ID1 competitively binds with APC/C^{Cdh1}, leading to reduced interaction of APC/C^{Cdh1} with AURKA, which then inhibited APC/C^{Cdh1}-mediated AURKA protein degradation and upregulated AURKA expression. Of note, certain studies have claimed that ID1 can also bind to various components of the 26S proteasome, such as the S5A subunit, which is important in the recognition and shuttling of the polyubiquitinated substrates to the proteasome (54-56). These effects may also block the AURKA proteasomal degradation, which needs further confirmation.

Myc is a crucial proto-oncogene that has been implicated in both tumor initiation and maintenance in most types of human cancer, and a number of studies have shown that HCC is dependent on Myc (40-42). Previous findings reported that AURKA regulates proteolytic turnover of MYCN in neuroblastoma (42), and a more recent study suggested that AURKA and Myc interact physically in TP53-altered cells (41). These previous studies encouraged us to clarify if Myc is the critical downstream molecule of the ID1/AURKA signaling pathway. It was identified that ID1 upregulated Myc activation in an AURKA-dependent manner, which was largely abolished by AKI. Further analysis demonstrated that AURKA transcriptionally activated Myc, which was consistent with previous findings that AURKA activates the Myc promoter (53). Furthermore, the present study demonstrated that AURKA also affected Myc protein turnover, implying that AURKA can regulate Myc expression at both the transcriptional and post-transcriptional levels, subsequently amplifying the Myc signaling pathway. Notably, unlike the AKI, MYC did not completely reverse ID1-induced chemoresistance, suggesting other mechanisms downstream of AURKA may be involved and need to be determined in the future.

However, there were several limitations of the current study. First, only oxaliplatin was used to investigate the role of ID1/AURKA/Myc signaling in HCC chemoresistance. Since sorafenib and lenvatinib are also first-line chemotherapy drugs for advanced HCC (30,57,58), future studies are required to explore the mechanisms underlying chemoresistance against sorafenib and lenvatinib, and whether ID1/AURKA/Myc

signaling is involved. Secondly, a larger sample size would be helpful to further confirm the association of ID1/AURKA with HCC prognosis. Thirdly, cells should be serum-starved for wound healing assays; however, 1% FBS was used in the present study. Furthermore, further studies are required to clarify other unknown downstream signaling underlying ID1/AURKA, which is ongoing in our laboratory.

In conclusion, the present study revealed the critical role of a novel ID1/AURKA/Myc signaling pathway in HCC malignant progression. Increase expression of ID1 induced HCC cells to exhibit highly malignant phenotypes, with enhanced metastatic ability and drug resistance, leading to HCC progression and poor prognosis. Specifically, ID1 upregulated AURKA expression by competitively binding with APC/C^{Cdh1}, thus inhibiting APC/C^{Cdh1}-mediated AURKA protein degradation. Increased AURKA subsequently amplified the Myc oncogenic signaling pathway at both the transcriptional and post-transcriptional levels. Based on the present results, targeting the ID1/AURKA/Myc regulatory axis could provide a novel promising therapeutic target that could improve the clinical outcome of advanced HCC.

Acknowledgements

Not applicable.

Funding

The present study was supported by the National Natural Science Foundation of China (grant nos. 81272565, 81502491 and 81600095) and the State Scholarship Fund of China (grant no. 201706100120).

Availability of data and materials

The datasets used and/or analyzed during the current study are available from the corresponding author on reasonable request.

Authors' contributions

ZR and MW conceived and designed this study. MW, YZ and CF performed all the experiments. XY, LZ, and TC collected the data and performed statistical analyses. XY and LZ provided optimal experimental protocols and materials. ZR and MW prepared the manuscript, with input from all authors. All authors provided critical feedback and helped shape the research, analysis and manuscript. All authors read and approved the final manuscript.

Ethics approval and consent to participate

The present study was approved by the Ethics Committee of the Zhongshan Hospital Affiliated with Fudan University, and all research strictly abided to the Declaration of Helsinki. All individuals involved in the study provided written informed consent.

Patient consent for publication

Not applicable.

Competing interests

The authors declare that they have no competing interests.

References

1. Bray F, Ferlay J, Soerjomataram I, Siegel RL, Torre LA and Jemal A: Global cancer statistics 2018: GLOBOCAN estimates of incidence and mortality worldwide for 36 cancers in 185 countries. *CA Cancer J Clin* 68: 394-424, 2018.
2. Cronin KA, Lake AJ, Scott S, Sherman RL, Noone AM, Howlander N, Henley SJ, Anderson RN, Firth AU, Ma J, *et al*: Annual Report to the Nation on the Status of Cancer, part I: National cancer statistics. *Cancer* 124: 2785-2800, 2018.
3. Tang ZY: Hepatocellular carcinoma--cause, treatment and metastasis. *World J Gastroenterol* 7: 445-454, 2001.
4. Llovet JM and Bruix J: Systematic review of randomized trials for unresectable hepatocellular carcinoma: Chemoembolization improves survival. *Hepatology* 37: 429-442, 2003.
5. Craig AJ, von Felden J, Garcia-Lezana T, Sarcognato S and Villanueva A: Tumour evolution in hepatocellular carcinoma. *Nat Rev Gastroenterol Hepatol* 17: 139-152, 2020.
6. Perk J, Iavarone A and Benezra R: Id family of helix-loop-helix proteins in cancer. *Nat Rev Cancer* 5: 603-614, 2005.
7. Sachdeva R, Wu M, Smiljanic S, Kaskun O, Ghannad-Zadeh K, Celebre A, Isaev K, Morrissy AS, Guan J, Tong J, *et al*: ID1 is critical for tumorigenesis and regulates chemoresistance in glioblastoma. *Cancer Res* 79: 4057-4071, 2019.
8. Huang YH, Hu J, Chen F, Lecomte N, Basnet H, David CJ, Witkin MD, Allen PJ, Leach SD, Hollmann TJ, *et al*: ID1 mediates escape from TGFβ tumor suppression in pancreatic cancer. *Cancer Discov* 10: 142-157, 2020.
9. Gumireddy K, Li A, Kossenkova AV, Cai KQ, Liu Q, Yan J, Xu H, Showe L, Zhang L and Huang Q: ID1 promotes breast cancer metastasis by S100A9 regulation. *Mol Cancer Res* 12: 1334-1343, 2014.
10. Román M, López I, Guruceaga E, Baraibar I, Ecay M, Collantes M, Nadal E, Vallejo A, Cadenas S, Miguel ME, *et al*: Inhibitor of differentiation-1 sustains mutant KRAS-driven progression, maintenance, and metastasis of lung adenocarcinoma via regulation of a FOSL1 network. *Cancer Res* 79: 625-638, 2019.
11. Fong S, Debs RJ and Desprez PY: Id genes and proteins as promising targets in cancer therapy. *Trends Mol Med* 10: 387-392, 2004.
12. Ao J, Meng J, Zhu L, Nie H, Yang C, Li J, Gu J, Lin Q, Long W, Dong X, *et al*: Activation of androgen receptor induces ID1 and promotes hepatocellular carcinoma cell migration and invasion. *Mol Oncol* 6: 507-515, 2012.
13. Yin X, Tang B, Li JH, Wang Y, Zhang L, Xie XY, Zhang BH, Qiu SJ, Wu WZ and Ren ZG: ID1 promotes hepatocellular carcinoma proliferation and confers chemoresistance to oxaliplatin by activating pentose phosphate pathway. *J Exp Clin Cancer Res* 36: 166, 2017.
14. Niu LL, Cheng CL, Li MY, Yang SL, Hu BG, Chong CCN, Chan SL, Ren J, Chen GG and Lai PBS: ID1-induced p16/IL6 axis activation contributes to the resistant of hepatocellular carcinoma cells to sorafenib. *Cell Death Dis* 9: 852, 2018.
15. Marumoto T, Zhang D and Saya H: Aurora-A - a guardian of poles. *Nat Rev Cancer* 5: 42-50, 2005.
16. Tang A, Gao K, Chu L, Zhang R, Yang J and Zheng J: Aurora kinases: Novel therapy targets in cancers. *Oncotarget* 8: 23937-23954, 2017.
17. Jeng YM, Peng SY, Lin CY and Hsu HC: Overexpression and amplification of Aurora-A in hepatocellular carcinoma. *Clin Cancer Res* 10: 2065-2071, 2004.
18. Tayyar Y, Jubair L, Fallaha S and McMillan NAJ: Critical risk-benefit assessment of the novel anti-cancer aurora kinase inhibitor alisertib (MLN8237): A comprehensive review of the clinical data. *Crit Rev Oncol Hematol* 119: 59-65, 2017.
19. Beltran H, Oromendia C, Danila DC, Montgomery B, Hoimes C, Szmulewitz RZ, Vaishampayan U, Armstrong AJ, Stein M, Pinski J, *et al*: A phase II trial of the Aurora Kinase A inhibitor Alisertib for patients with castration-resistant and neuroendocrine prostate cancer: Efficacy and biomarkers. *Clin Cancer Res* 25: 43-51, 2019.
20. Hasskarl J, Duensing S, Manuel E and Münger K: The helix-loop-helix protein ID1 localizes to centrosomes and rapidly induces abnormal centrosome numbers. *Oncogene* 23: 1930-1938, 2004.

21. Cowley DO, Rivera-Pérez JA, Schliekelman M, He YJ, Oliver TG, Lu L, O'Quinn R, Salmon ED, Magnuson T and Van Dyke T: Aurora-A kinase is essential for bipolar spindle formation and early development. *Mol Cell Biol* 29: 1059-1071, 2009.
22. Nikonova AS, Aptsaturov I, Serebriiskii IG, Dunbrack RL Jr and Golemis EA: Aurora A kinase (AURKA) in normal and pathological cell division. *Cell Mol Life Sci* 70: 661-687, 2013.
23. Meraldi P, Honda R and Nigg EA: Aurora-A overexpression reveals tetraploidization as a major route to centrosome amplification in p53^{-/-} cells. *EMBO J* 21: 483-492, 2002.
24. Man C, Rosa J, Yip YL, Cheung AL, Kwong YL, Doxsey SJ and Tsao SW: Id1 overexpression induces tetraploidization and multiple abnormal mitotic phenotypes by modulating aurora A. *Mol Biol Cell* 19: 2389-2401, 2008.
25. Marrero JA, Kulik LM, Sirlin CB, Zhu AX, Finn RS, Abecassis MM, Roberts LR and Heimbach JK: Diagnosis, staging, and management of hepatocellular carcinoma: 2018 practice guidance by the american association for the study of liver diseases. *Hepatology* 68: 723-750, 2018.
26. Llovet JM, Fuster J and Bruix J; Barcelona-Clínic Liver Cancer Group: The Barcelona approach: Diagnosis, staging, and treatment of hepatocellular carcinoma. *Liver Transpl* 10 (Suppl 1): S115-S120, 2004.
27. Li Y, Tian B, Yang J, Zhao L, Wu X, Ye SL, Liu YK and Tang ZY: Stepwise metastatic human hepatocellular carcinoma cell model system with multiple metastatic potentials established through consecutive in vivo selection and studies on metastatic characteristics. *J Cancer Res Clin Oncol* 130: 460-468, 2004.
28. Jawhar NM: Tissue Microarray: A rapidly evolving diagnostic and research tool. *Ann Saudi Med* 29: 123-127, 2009.
29. Detre S, Saclani Jotti G and Dowsett M: A 'quickscore' method for immunohistochemical semiquantitation: Validation for oestrogen receptor in breast carcinomas. *J Clin Pathol* 48: 876-878, 1995.
30. Zhang P, Wen F and Li Q: FOLFOX4 or sorafenib as the first-line treatments for advanced hepatocellular carcinoma: A cost-effectiveness analysis. *Dig Liver Dis* 48: 1492-1497, 2016.
31. Qin S, Bai Y, Lim HY, Thongprasert S, Chao Y, Fan J, Yang TS, Bhudhisawasdi V, Kang WK, Zhou Y, *et al*: Randomized, multicenter, open-label study of oxaliplatin plus fluorouracil/leucovorin versus doxorubicin as palliative chemotherapy in patients with advanced hepatocellular carcinoma from Asia. *J Clin Oncol* 31: 3501-3508, 2013.
32. Slevin M, Kumar S and Gaffney J: Angiogenic oligosaccharides of hyaluronan induce multiple signaling pathways affecting vascular endothelial cell mitogenic and wound healing responses. *J Biol Chem* 277: 41046-41059, 2002.
33. Livak KJ and Schmittgen TD: Analysis of relative gene expression data using real-time quantitative PCR and the 2⁻(Delta Delta C(T)) Method. *Methods* 25: 402-408, 2001.
34. Li H, Li CW, Li X, Ding Q, Guo L, Liu S, Liu C, Lai CC, Hsu JM, Dong Q, *et al*: MET inhibitors promote liver tumor evasion of the immune response by stabilizing PDL1. *Gastroenterology* 156 (2019): 1849-1861e13, 2019.
35. Guichard C, Amadio G, Imbeaud S, Ladeiro Y, Pelletier L, Maad IB, Calderaro J, Bioulac-Sage P, Letexier M, Degos F, *et al*: Integrated analysis of somatic mutations and focal copy-number changes identifies key genes and pathways in hepatocellular carcinoma. *Nat Genet* 44: 694-698, 2012.
36. Lamb JR, Zhang C, Xie T, Wang K, Zhang B, Hao K, Chudin E, Fraser HB, Millstein J, Ferguson M, *et al*: Predictive genes in adjacent normal tissue are preferentially altered by sCNV during tumorigenesis in liver cancer and may rate limiting. *PLoS One* 6: e20090, 2011.
37. Taguchi S, Honda K, Sugiura K, Yamaguchi A, Furukawa K and Urano T: Degradation of human Aurora-A protein kinase is mediated by hCdh1. *FEBS Lett* 519: 59-65, 2002.
38. Walter AO, Seghezzi W, Korver W, Sheung J and Lees E: The mitotic serine/threonine kinase Aurora2/AIK is regulated by phosphorylation and degradation. *Oncogene* 19: 4906-4916, 2000.
39. Li B, Xu WW, Guan XY, Qin YR, Law S, Lee NPY, Chan KT, Tam PY, Li YY, Chan KW, *et al*: Competitive binding between Id1 and E2F1 to Cdc20 regulates E2F1 degradation and thymidylate synthase expression to promote esophageal cancer chemoresistance. *Clin Cancer Res* 22: 1243-1255, 2016.
40. Dang CV: MYC on the path to cancer. *Cell* 149: 22-35, 2012.
41. Dauch D, Rudalska R, Cossa G, Nault JC, Kang TW, Wuestefeld T, Hohmeyer A, Imbeaud S, Yevsa T, Hoenicke L, *et al*: A MYC-aurora kinase A protein complex represents an actionable drug target in p53-altered liver cancer. *Nat Med* 22: 744-753, 2016.
42. Otto T, Horn S, Brockmann M, Eilers U, Schüttrumpf L, Popov N, Kenney AM, Schulte JH, Beijersbergen R, Christiansen H, *et al*: Stabilization of N-Myc is a critical function of Aurora A in human neuroblastoma. *Cancer Cell* 15: 67-78, 2009.
43. Chuma M, Terashita K and Sakamoto N: New molecularly targeted therapies against advanced hepatocellular carcinoma: From molecular pathogenesis to clinical trials and future directions. *Hepatol Res* 45: E1-E11, 2015.
44. Kononen J, Bubendorf L, Kallioniemi A, Bärklund M, Schraml P, Leighton S, Torhorst J, Mihatsch MJ, Sauter G and Kallioniemi OP: Tissue microarrays for high-throughput molecular profiling of tumor specimens. *Nat Med* 4: 844-847, 1998.
45. Alkushi A: Validation of tissue microarray biomarker expression of breast carcinomas in Saudi women. *Hematol Oncol Stem Cell Ther* 2: 394-398, 2009.
46. Graham AD, Faratian D, Rae F and Thomas JS: Tissue microarray technology in the routine assessment of HER-2 status in invasive breast cancer: A prospective study of the use of immunohistochemistry and fluorescence in situ hybridization. *Histopathology* 52: 847-855, 2008.
47. Drev P, Grazio SF and Bracko M: Tissue microarrays for routine diagnostic assessment of HER2 status in breast carcinoma. *Appl Immunohistochem Mol Morphol* 16: 179-184, 2008.
48. Hanahan D and Weinberg RA: Hallmarks of cancer: The next generation. *Cell* 144: 646-674, 2011.
49. Cho Y, Cho EJ, Lee J-H, Yu SJ, Kim YJ, Kim CY and Yoon JH: Fucoidan-induced ID-1 suppression inhibits the in vitro and in vivo invasion of hepatocellular carcinoma cells. *Biomed Pharmacother* 83: 607-616, 2016.
50. Yan M, Wang C, He B, Yang M, Tong M, Long Z, Liu B, Peng F, Xu L, Zhang Y, *et al*: Aurora-A Kinase: A potent oncogene and target for cancer therapy. *Med Res Rev* 36: 1036-1079, 2016.
51. Cammareri P, Scopelliti A, Todaro M, Eterno V, Francescangeli F, Moyer MP, Agrusa A, Dieli F, Zeuner A, Stassi G, *et al*: Aurora-A is essential for the tumorigenic capacity and chemoresistance of colorectal cancer stem cells. *Cancer Research* 70: 4655-4665, 2010.
52. Wan XB, Long ZJ, Yan M, Xu J, Xia LP, Liu L, Zhao Y, Huang XF, Wang XR, Zhu XF, *et al*: Inhibition of Aurora-A suppresses epithelial-mesenchymal transition and invasion by downregulating MAPK in nasopharyngeal carcinoma cells. *Carcinogenesis* 29: 1930-1937, 2008.
53. Zheng F, Yue C, Li G, He B, Cheng W, Wang X, Yan M, Long Z, Qiu W, Yuan Z, *et al*: Nuclear AURKA acquires kinase-independent transactivating function to enhance breast cancer stem cell phenotype. *Nat Commun* 7: 10180, 2016.
54. Hasskarl J, Mern DS and Mürger K: Interference of the dominant negative helix-loop-helix protein ID1 with the proteasomal subunit S5A causes centrosomal abnormalities. *Oncogene* 27: 1657-1664, 2008.
55. Geng F, Wenzel S and Tansey WP: Ubiquitin and proteasomes in transcription. *Annu Rev Biochem* 81: 177-201, 2012.
56. Hershko A and Ciechanover A: The ubiquitin system. *Annu Rev Biochem* 67: 425-479, 1998.
57. Bruix J and Sherman M; American Association for the Study of Liver Diseases: Management of hepatocellular carcinoma: An update. *Hepatology* 53: 1020-1022, 2011.
58. Peck-Radosavljevic M: Drug therapy for advanced-stage liver cancer. *Liver Cancer* 3: 125-131, 2014.